Supplement of Atmos. Chem. Phys., 19, 5451–5465, 2019
https://doi.org/10.5194/acp-19-5451-2019-supplement

Atmospheric Chemistry and Physics
Open Access
EGU

Supplement of

The importance of crystalline phases in ice nucleation by volcanic ash

Elena C. Maters et al.

Correspondence to: Elena C. Maters (e.c.maters@leeds.ac.uk)

Supplementary Material

Table S1. Bulk chemical composition of the tephra and glass samples used in this study, determined by X-ray fluorescence and normalised to 100 wt.% (excluding loss on ignition).

Sample[a]	SiO_2	Al_2O_3	Fe_2O_3	MgO	CaO	Na_2O	K_2O	TiO_2	MnO	P_2O_5
Tephra										
LIP_{teph}	75.5	13.0	1.6	0.0	0.8	3.7	5.2	0.1	0.1	0.0
COL_{teph}	61.7	18.9	4.4	1.9	5.9	4.9	1.4	0.5	0.1	0.2
TUN_{teph}	59.4	17.5	6.3	3.2	6.5	4.1	1.9	0.9	0.1	0.2
CID_{teph}	62.4	17.4	4.2	0.9	1.5	7.0	5.3	0.9	0.2	0.2
AST_{teph}	59.5	18.9	4.2	0.9	3.2	4.0	8.6	0.5	0.1	0.2
NUO_{teph}	60.3	19.9	3.3	0.2	1.9	6.4	7.2	0.4	0.2	0.0
LAC_{teph}	59.0	21.3	2.5	0.3	1.1	9.4	5.6	0.3	0.3	0.1
ETN_{teph}	47.7	17.3	11.3	5.2	10.4	3.6	2.0	1.7	0.2	0.6
KIL_{teph}	50.4	13.2	12.4	8.0	10.4	2.2	0.5	2.4	0.2	0.2
Glass										
LIP_{glass}	75.4	13.0	1.7	0.1	0.8	3.7	5.2	0.1	0.1	0.0
COL_{glass}	61.8	18.8	4.3	2.0	5.9	4.8	1.4	0.5	0.1	0.2
TUN_{glass}	59.4	17.5	6.3	3.2	6.5	4.1	1.9	0.9	0.1	0.2
CID_{glass}	62.3	17.4	4.4	0.9	1.7	6.9	5.2	0.9	0.2	0.2
AST_{glass}	59.6	18.9	4.2	0.9	3.2	3.9	8.5	0.5	0.1	0.2
NUO_{glass}	60.6	20.0	3.3	0.2	1.9	6.2	7.0	0.4	0.2	0.0
LAC_{glass}	59.0	21.4	2.5	0.3	1.1	9.4	5.5	0.3	0.4	0.1
ETN_{glass}	47.7	17.4	11.2	5.2	10.4	3.6	2.0	1.7	0.2	0.6
KIL_{glass}	50.6	13.1	12.1	7.9	10.7	2.2	0.4	2.4	0.2	0.2

[a]Sample codes are listed in Table 1.

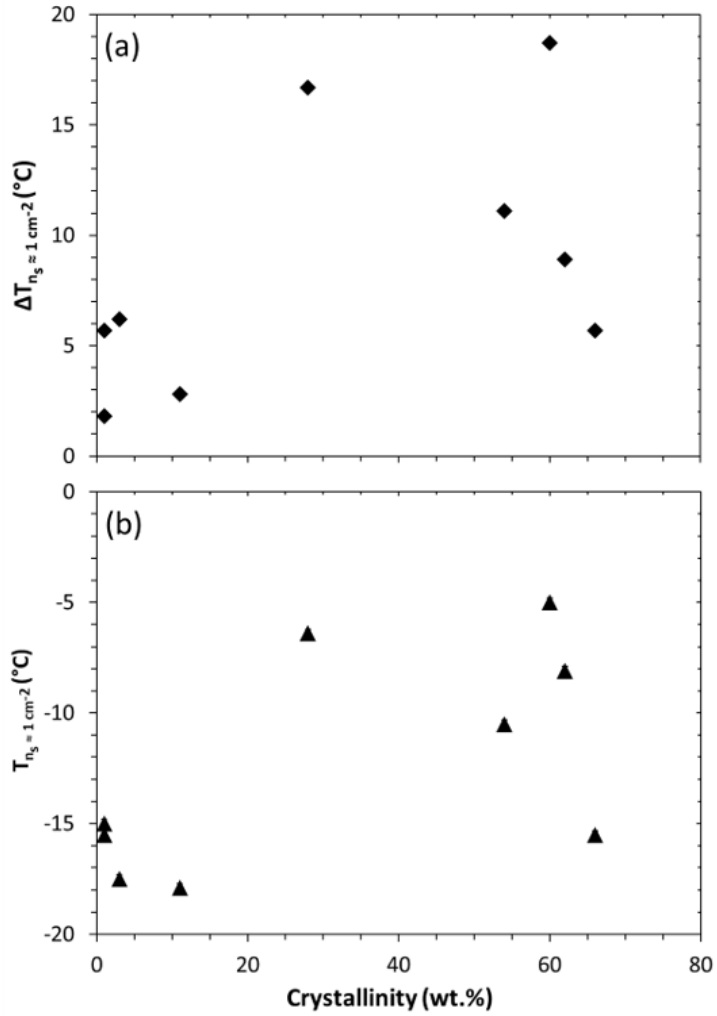

Figure S1. (a) The difference in INA ($\Delta T_{n_s \approx 1\ cm^{-2}}$) between the tephra and glass in each pair versus the crystallinity of the tephra, and (b) the INA ($T_{n_s \approx 1\ cm^{-2}}$) of the tephra versus the crystallinity of the tephra. Note that crystallinity below the XRD quantification limit (LIP_{teph}, CID_{teph}) is plotted at 1 wt.%. Ice nucleation experiments were conducted with 1 wt.% suspensions of tephra or glass in water. The uncertainty in $T_{n_s \approx 1\ cm^{-2}}$ is shown as error bars (note that these are obscured by the data symbols).

Text S1. Electron microprobe analysis of the tephra samples was performed using a Cameca SX-100 instrument equipped with a LaB_6 cathode. A 10 µm focused beam was used at an accelerating voltage of 15 keV and a current of 5 nA to analyse at least five points for each crystalline phase in the tephra samples. Calibration was done on the following standard materials: albite - Na, Si; periclase - Mg; orthoclase - K, Al; wollastonite - Ca, Si; Fe_2O_3 - Fe; Cr_2O_3 - Cr; ilmenite - Ti; bustamite - Mn; apatite - P; vanadinite - Cl; anhydrite - S. Elemental detection limits in parts per million are as follows: Si - 786, Al - 655, Fe - 1573, Mg - 501, Ca - 747, Na - 973, K - 711, Ti - 894, Mn - 1401, P - 568, Cr - 1286, S - 767, Cl - 955.

Table S2. Average chemical composition of feldspar in tephra samples used in this study, determined by electron microprobe analysis and expressed in wt.%.

Sample[a]		**SiO_2**	**Al_2O_3**	**Fe_2O_3**	**MgO**	**CaO**	**Na_2O**	**K_2O**	**TiO_2**	**MnO**	**P_2O_5**	**Cr_2O_3**	**SO_3**	**Cl**	**Total**	**Na_2O/CaO in *pl***	**K_2O/Na_2O in *al***
COL_{teph}	*pl*	54.2	28.1	0.76	0.05	10.8	5.6	0.22	<d.l.	<d.l.	<d.l.	-	-	-	99.7	0.5	-
TUN_{teph}	*pl*	55.7	27.4	1.1	0.10	10.9	5.3	0.44	0.09	<d.l.	<d.l.	<d.l.	<d.l.	<d.l.	101.0	0.5	-
AST_{teph}	*pl*	54.6	26.9	0.68	<d.l.	9.6	4.7	2.5	0.04	<d.l.	<d.l.	<d.l.	-	<d.l.	99.0	0.5	-
	al	63.7	19.3	0.40	<d.l.	0.84	2.5	12.4	0.10	<d.l.	-	<d.l.	<d.l.	-	99.2	-	5.0
NUO_{teph}	*al*	64.0	20.7	0.85	<d.l.	2.1	5.9	7.0	0.16	<d.l.	<d.l.	<d.l.	<d.l.	<d.l.	100.7	-	1.2
LAC_{teph}	*al*	63.9	20.2	0.76	0.05	1.3	4.8	9.2	0.14	<d.l.	<d.l.	<d.l.	<d.l.	<d.l.	100.4	-	1.9
ETN_{teph}	*pl*	48.5	32.4	1.2	0.08	15.9	2.5	0.22	0.09	<d.l.	<d.l.	<d.l.	<d.l.	-	100.9	0.2	-
KIL_{teph}	*pl*	50.3	31.0	1.0	0.17	15.4	3.0	0.12	0.11	-	<d.l.	-	<d.l.	-	101.1	0.2	-

[a]Sample codes are listed in Table 1. *pl* = plagioclase (Na-/Ca-) feldspar, *al* = alkali (K-) feldspar. d.l. = detection limit.

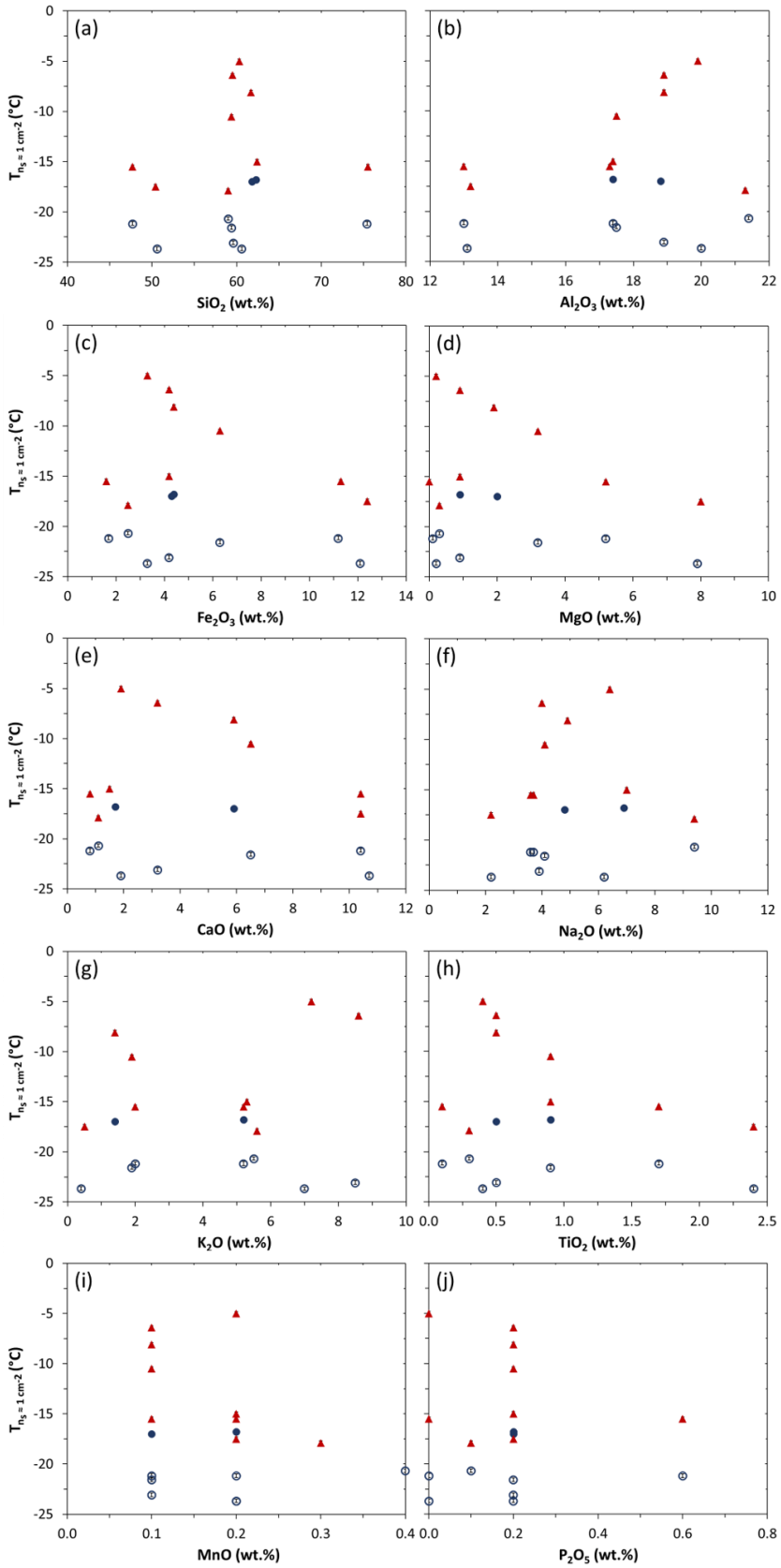

Figure S2. The INA ($T_{n_s \approx 1\ cm^{-2}}$) of the tephra (red triangles) and glass (blue circles) versus their (a) SiO_2, (b) Al_2O_3, (c) Fe_2O_3, (d) MgO, (e) CaO, (f) Na_2O, (g) K_2O, (h) TiO_2, (i) MnO, and (j) P_2O_5 contents. The open blue circles correspond to glasses (all except CID_{glass} and COL_{glass}) for which ice nucleation cannot be distinguished from that induced by the background water. Ice nucleation experiments were conducted with 1 wt.% suspensions of tephra or glass in water. The uncertainty in $T_{n_s \approx 1\ cm^{-2}}$ is shown as error bars (note that these are obscured by the data symbols).